SOUTHERN GALAXIES. V. ISOPHOTOMETRY OF THE LARGE BARRED SPIRAL NGC 4945

G. DE VAUCOULEURS
Department of Astronomy, University of Texas
Received October 18, 1963

ABSTRACT

Isophotes and photometric parameters are derived for the large SB(s)d spiral NGC 4945 from a Mount Stromlo 30-inch reflector plate. The total apparent photographic magnitude $m_T = 9.85$ (with provisional zero point) and maximum dimensions $24' \times 6'$ (at the threshold $\mu_m = 27.3$ mag/sec^2 = 0.95 $\odot$/pc^2) correspond to $M_T = -19.15$ and $D_m = 26.5$ kpc, if $m - M = 29.0$ and $\Delta = 3.8$ Mpc. The galactic absorption $A \simeq 1.1$ mag is uncertain at the low latitude $b^{II} = +13°.5$ of this object. The major axis is in p.a $\theta = 42°$; the mean axis ratio of the outer regions $q = \langle b/a \rangle = 0.193$ corresponds to an inclination $i = 82°$, if $q_0 = 0.13$. The equivalent radius is $r_e^* = 2'.13 = 2.34$ kpc, the effective surface brightness $\mu_e = 22.80$ mag sec^{-2} = 58 $\odot$/pc^2, and the mean luminosity gradient in the roughly exponential outer regions $G(a) = -0.13$ min^{-1} = -0.12 kpc^{-1}. The continuum radio emission is discussed; the apparent radio index is $m_r - m_p = 0.0$; the index corrected for both galactic and internal absorption is $m_r - m_p = +1.3$, which is about average for Sc–Sd galaxies.

I. INTRODUCTION

This is the fourth paper in a series on the surface photometry of bright southern galaxies photographed between 1952 and 1956 with the 30-inch and 74-inch reflectors of Mount Stromlo Observatory (de Vaucouleurs 1956*b;* G. and A. de Vaucouleurs 1961). The definitions of the photometric parameters will be found in an article of "Problems of Extragalactic Research" (de Vaucouleurs 1962) and details of the observations and reductions in previous papers of this series (de Vaucouleurs 1961 [Paper I], 1963*a* [Paper III]), 1963*b* (Paper IV), and especially Paper II (de Vaucouleurs and J. Page 1962).

II. OBSERVATIONS

Only one good plate (RN-50, February 11, 1953) in blue light (103a-O, no filter, exp. 1 hr.) taken with the 30-inch reflector (stopped to 20 inches = $f/6$) was available for this study of NGC 4945, but the small scale (1 mm = 67″) is not a serious difficulty for such a large object. The estimated surface brightness of the night sky μ_s(pg) = 21.78 per sq. sec of arc computed from the data of Elvey and Roach (1937) for the appropriate ecliptic and galactic coordinates and zenith distance (sec $z = 1.03$) is used as a convenient arbitrary unit and *provisional* zero point of surface intensity $I = i/i_s$ (see Paper II). Because of the day-to-day fluctuations of the airglow, no great accuracy is expected; occasional photoelectric checks of the B surface brightness of the night sky at Mount Stromlo and elsewhere suggest that in a period of low solar activity the fluctuations of i_s may introduce a *probable error* of the order of 0.1–0.2 mag. in μ_s and in the photometric parameters which depend on it (m, M, $\mathfrak{L}$). This uncertainty will be removed by photoelectric observations of parts of the galaxy through various field apertures and by integration of the photographic isophotes within these apertures. In the meantime photographic magnitudes with p.e.'s of ± 0.2 mag. are sufficient for comparison with radio observations which are subject to calibration errors of the same order.

III. DESCRIPTION

NGC 4945 is a large, but little-known late-type spiral at the low galactic latitude $b^{II} = +13°.5$ in Centaurus. It forms a wide pair at 32′ with an elliptical companion NGC 4976, type E5, and possibly belongs to a loose group including NGC 5236 (M83),

5253, and perhaps NGC 5128 (de Vaucouleurs 1956*a*). A small, faint object 17′ south-following the center of NGC 4945 may be a dwarf irregular companion.

The small angle between the plane of the system and the line of sight makes its classification a little uncertain; the classification SB?(s)c: in the Reynolds survey is now revised to SB(s)cd or possibly SAB(s)cd because of the strong asymmetry and inconspicuous nucleus (Figs. 1, 2), the same characteristics that were noted in NGC 1313 (Paper III). The bar, much dimmed by obscuring clouds on the near (south-following) side of the system, is close to the minor axis in the projection, i.e., points toward the Sun.

This orientation and the large angular dimensions (over 20′ × 5′ [see Sec. VI]) make NGC 4945 a promising object for a detailed study of the large-scale streaming motions of the gas along the bar. Such motions were recently detected at McDonald Observatory in several smaller barred spirals (G. and A. de Vaucouleurs 1962*a*, *b*). The main elements of NGC 4945, listed in Table 1, are taken mainly from the Mount Stromlo survey (de Vaucouleurs 1956*b*); note the correction to the NGC coordinates (after R. Shobbrook, quoted by Mathewson and Rome 1963).

TABLE 1

ELEMENTS OF NGC 4945*

α(1950)	13^h02^m4	Inner dimensions	$D_i \times d_i$	15′ × 2′.5	1
δ(1950)	−49°13′	Outer dimensions	$D_0 \times d_0$	20′: × 4′:	1
l_I, b_I	273°.28, +12°.93	...	.	. ..	.
l_{II}, b_{II}	305°.25, +13°.32	Mean axis ratio	R_m	0 18	1
L, B	165°.9, −10°.2	Concentration index	C	0.66:	1
Type	SB(s)cd	"Face-on" diameter	$D(0)$	7′.95	2

* The sources are as follows: (1) Mount Stromlo 30-inch reflector (de Vaucouleurs 1956*b*); (2) *Reference Catalogue of Bright Galaxies* (in preparation)

IV. DISTANCE

There is no trace of resolution into stars on the 30-inch plate (Fig. 1), hence $m_* \gg 19$ and $m - M \gg 28$. The "face-on" diameter of NGC 4945 is log $D(0) = 0.90$; by comparison with the corresponding values for NGC 55, 1313, and 4631 (Papers I, III; G. and A. de Vaucouleurs 1963) this leads to $m_0 - M = 27.7$, 27.95, and 28.05; the adopted value is $m_0 - M = 27.9$. The corresponding distance is $\Delta = 3.8$ Mpc and the scale factor 1′ = 1.10 kpc. At $b = +13°.5$ the cosecant law gives $A \simeq 1.1$ mag.; and the apparent modulus is $m - M \simeq 29.0$ with a rather large margin of uncertainty.

V. ISOPHOTES

The isophotes from the 30-inch plate No. 50 are shown in Figure 3; two scanning spot sizes were used as indicated by the hatched disks. The position of the nucleus is not definite; it may be the brightest point inside contour No. 1 through which the minor axis scan No. 2 was taken. The longest axis of the nebula, however, along which scan No. 3 was taken is in p.a. $\theta = 42° \pm 1°$ (1875) and it crosses the minor axis 24″ southeast of the brightness peak. The ellipticity curve is shown in Figure 4 for which axis No. 3 was taken as the major axis. The mean axis ratio in the range $3'.5 < a < 11'.5$ is $q = 5$ $\langle b/a \rangle = 0.193$. Obviously the statistical average value of the true axis ratio $q_0 = 0.2$ often used for spirals (Holmberg 1958) does not apply here. Since $q_0 > 0.0$, a lower limit of the inclination is $i > 79°$; if $q_0 \simeq 0.1$, $i \simeq 80°.5$. The stronger arm emerging from the end of the bar north of the center crosses major axis No. 3 about 295″ NE. and 570″ SW. from axis No. 2 and its minor axis is about 115″; if it is circular in its own plane, this axis ratio $b/a = 0.132$ corresponds to $i = 82°.5$. The value $i = 82° \pm 1°$ (p.e.), corresponding to $q_0 \simeq 0.135$, may be adopted.

FIG. 1.—NGC 4945. 30-inch reflector, Mount Stromlo Observatory; 1 mm = 8″.0; north at top, east at left.

FIG. 2.—NGC 4945. 30-inch reflector, central regions, low-contrast print. 1 mm = 5″.8; north at top, east at left.

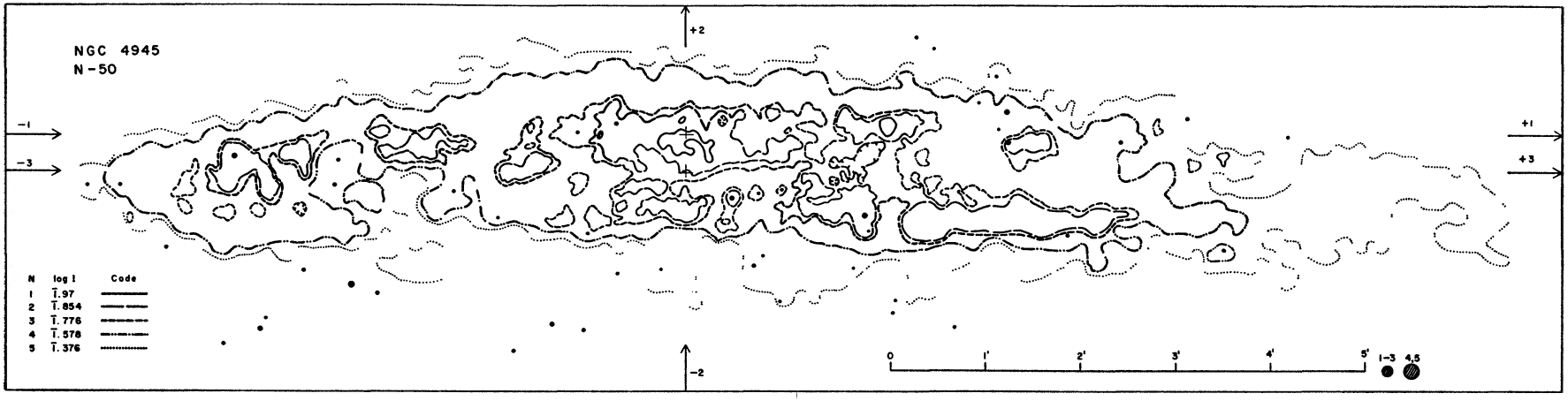

FIG. 3.—Isophotes of brighter regions. The locations of the photometric cross-sections of Figs. 5–7 are marked

VI. LUMINOSITY PROFILES

The luminosity profiles along axes Nos. 1 and 2 through the presumed nucleus and axis No. 3 (major axis) are shown in Figures 5–7. The actual measured points rather than a smoothed curve are shown in the central sections of axes Nos. 1 and 3, where the scatter is due to real structural details of the nebula rather than to plate grain; the dashed sections are smoothed interpolations of the outer regions where the scatter is dominated by plate grain. Note the strong asymmetry of the nebula along the major axis (cf. Fig. 1). The peak brightness $\mu_0 \simeq 21.8$ mag sec^{-2} is not seriously limited by resolving power; it is hardly higher than the brightness μ_s of the night sky. The threshold brightness for the luminosity profiles $\mu \simeq 26.3$ mag sec^{-2} is higher than usual because of the

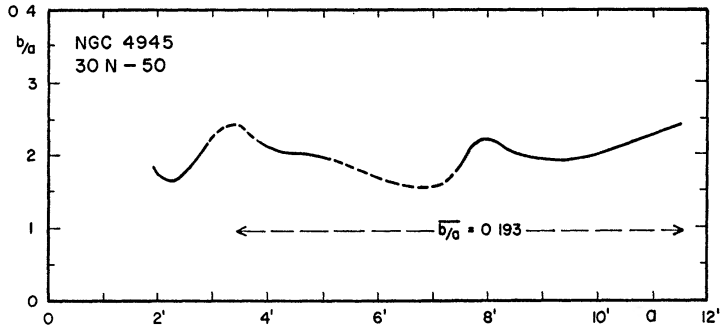

FIG. 4.—Mean axis ratio of isophotes along axes 2 and 3 versus axis 3 semidiameter (major axis)

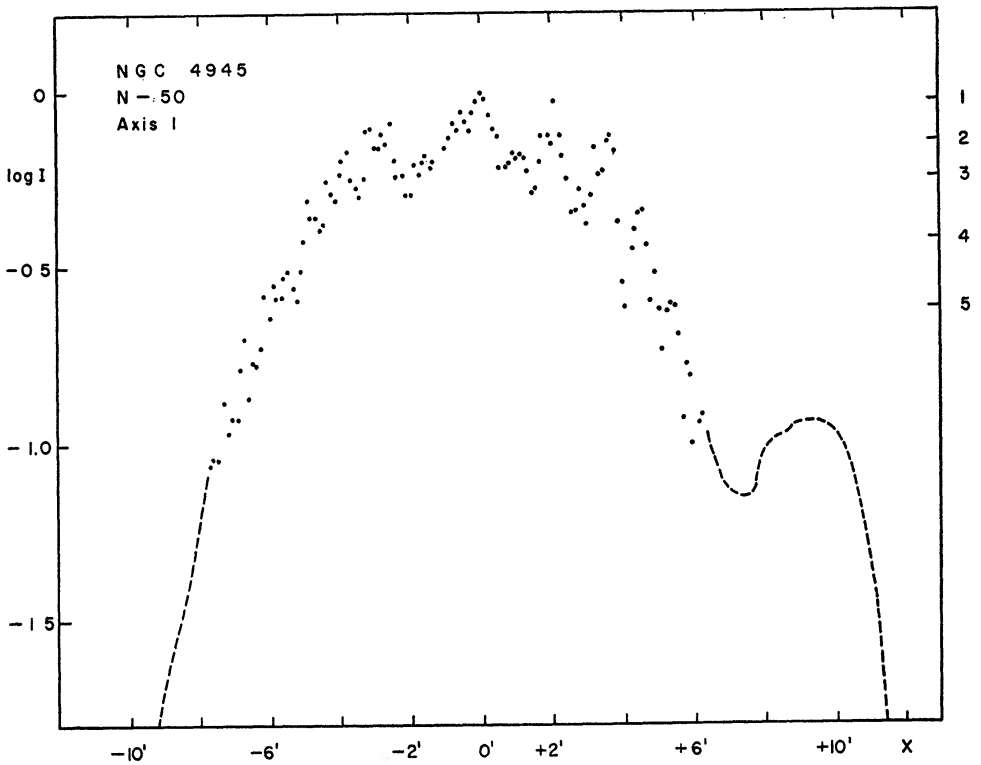

FIG. 5.—Luminosity profile along axis No. 1 through apparent nucleus. Individual measured points are shown in central region where most of the scatter reflects true fine structure rather than plate grain.

crowded star field and difficulties caused by scattered light from the 5th-mag. star ξ_1 Cen which is 14′ west of the south-preceding end of NGC 4945. The maximum dimensions derived from the scans of axes Nos. 3 and 2 are at least 21′.5 × 4′.9 and possibly 25′.9 and 6′.9; we shall adopt $D_m \times d_m = (24' \pm 2') \times (6' \pm 1') = 26.5 \times 6.6$ kpc for an estimated threshold brightness $\mu_m \simeq 27.3$ mag sec^{-2}.

The equivalent luminosity profile is shown in Figure 8; the absence of a sharp peak in the center is noteworthy. The roughly exponential outer parts have a mean gradient

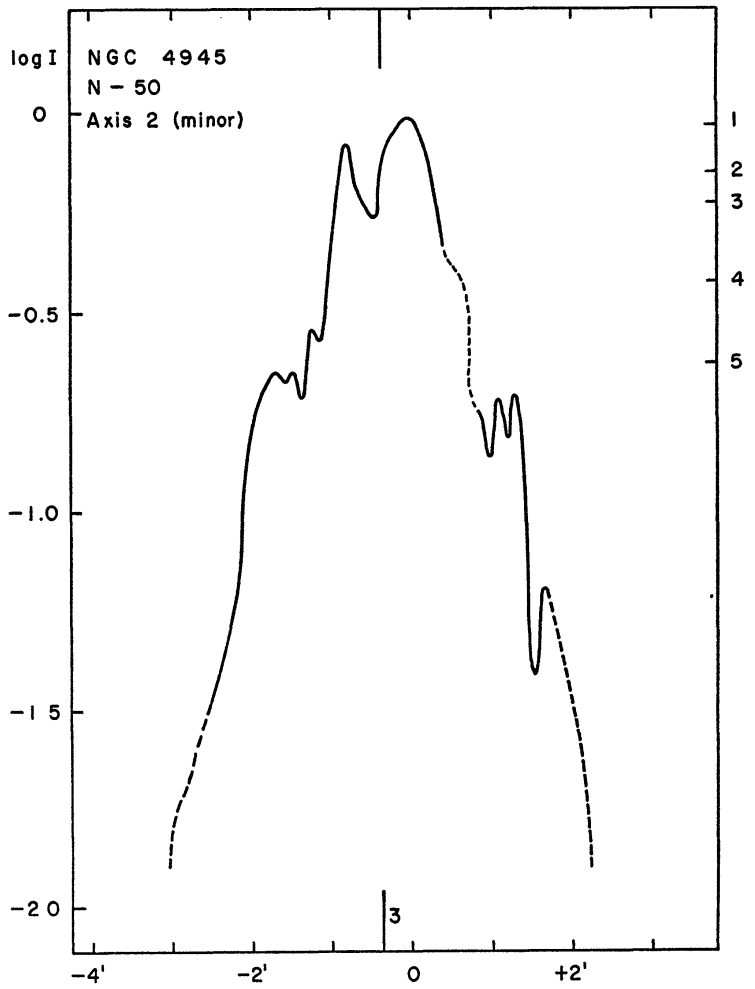

FIG. 6.—Luminosity profile along axis No. 2 (minor axis). Dashed parts are uncertain

$G(a) = -0.13$ min^{-1} $= -0.12$ kpc^{-1} and an equivalent gradient $G(r^*) = -0.405$ min^{-1} $= -0.37$ kpc^{-1}; this is close to the corresponding values for NGC 1313 (Paper III). Note that the extrapolated central brightness of the exponential component $\mu(0) = 21.5$: mag sec^{-2} is greater than the observed peak brightness; this may be caused by obscuration in the central regions.

VII. INTEGRATED LUMINOSITY

The mean and integrated luminosity distributions are given in Table 2. The extrapolated luminosity of the regions of surface brightness $\log I < -2.0$ is 0.26 unit or 1.6 per cent of the total luminosity $L_T = 16.45$, corresponding to $m_T = 9.85$, if $\mu_s = 12.89$

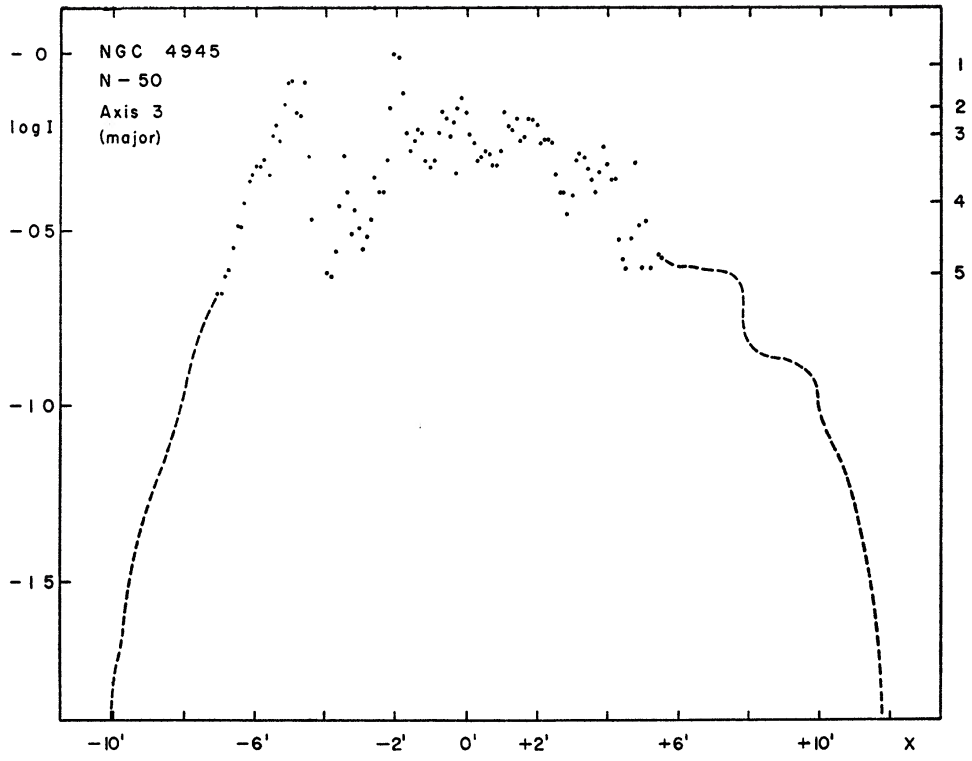

FIG 7.—Luminosity profile along axis No. 3 (major axis). Same remark as in Fig. 5

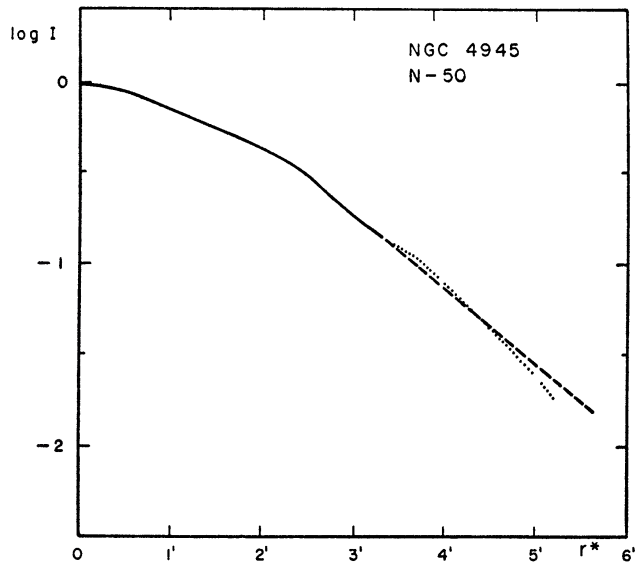

FIG. 8.—Equivalent luminosity profile *Continuous and dotted line*, observed (smoothed); *dashed line*, exponential approximation of outer part.

mag min^{-2}. The Shapley-Ames magnitude was $m_H = 9.2$:, uncertain because of the large size and low surface brightness. If $m - M = 29.0$, the absolute magnitude is $M_T = -19.15$ or about 0.4 mag. brighter than NGC 1313 and 1.0 mag. brighter than the Large Magellanic Cloud. The relative integrated luminosity curve is shown in Figure 9; the equivalent effective radius is $r_e^* = 2'.13 = 2.35$ kpc where $\mu_e = 22.80$ mag sec^{-2}. Other photometric parameters are listed in Table 3. The mean surface brightness inside the effective isophote is $\mu_e' = 13.49$ mag min^{-2}, about 1 mag. fainter than in NGC 1313 and the same as in NGC 55.

TABLE 2

MEAN LUMINOSITY DISTRIBUTION IN NGC 4945*

μ	log I	A	$P=\bar{I}\times\Delta A$	$k(r)$	r^*	a	b/a	α	ρ^*	log J
21 80	−0 01	0		0	0	0		0	0	+0 41
			1 24							
22 03	−0 1	1 41		0 075	0 67	1 5:		0 33	0 31	+0 32
			2 20							
22 28	−0 2	4 52		0 209	1 20	2 4	0 17	0 53	0 56	+0 22
			2 32							
22 53	−0 3	8 63		0 350	1 66	3 4	24:	0 75	0 78	+0 12
			2 22							
22 78	−0 4	13 59		0 485	2 08	4 2:	21	0 93:	0 98	+0 02
			1 60							
23 03	−0 5	18 10		0 582	2 40	4 5:	18	1 00:	1 13	−0 08
			1 20							
23 28	−0 6	22 35		0 655	2 67	5 0	19	1 10	1 25	−0 18
			0 99							
23 53	−0 7	26 75		0 715	2 92	6 5:	20:	1 44:	1 37	−0 28
			0 92							
23 78	−0 8	32 0		0 766	3 20	7 4:	18	1 64:	1 50	−0 38
			0 89							
24 03	−0 9	38 3		0 820	3 49	8 1:	22:	1 80:	1 64	−0 48
			0 57							
24 28	−1 0	43 4		0 855	3 72	8 7:	20	1 93:	1 76	−0 58
			0 45							
24 53	−1 1	48 4		0 881	3 93	9 2:	19	2 04:	1 84	−0 68
			0 40							
24 78	−1 2	54 0		0 905	4 14	9 6:	19	2 13:	1 94	−0 78
			0 30							
25 03	−1 3	59 4		0 924	4 35	9 8:	19	2 17:	2 04	−0 88
			0 27							
25 28	−1 4	65 4		0 940	4 56	10 2:	20	2 26:	2 14	−0 98
			0 21							
25 53	−1 5	71 3		0 953	4 76	10 5:	21	2 33:	2 24	−1 08
			0 17							
25 78	−1 6	77 2		0 964	4 96	10 8:	22	2 4::	2 33	−1 18
			0 12							
26 03	−1 7	82 9		0 970	5 14	11 1::	23:	2 45::	2 42	−1 28
			0 11							
26 28	−1 8	89 0		0 976	5 31	11 4::	23:	2 5::	2 49	−1 38
			0 07							
26 53	−1 9	94 2		0 981	5 47	11 7::	24:	2 6::	2 57	−1 48
			0 05							
26 78	−2 0	98 8		0 985	5 62	12 ::	0 24:	2 65::	2 64	−1 58
			0 26:							
∞	−∞			1						

* Units: μ in mag sec^{-2}, $I = 1$ for $\mu = \mu_s = 22$ 11; A in sq min; $\alpha = a/a_e$; $\rho^* = r^*/r_e^*$; $J = 1$ for $\mu = \mu_e = 22$ 80 mag sec^{-2}.

VIII. RADIO EMISSION

The continuous radio emission of NGC 4945 first detected by Mills at 85 Mc/s (Mills 1955; Mills, Slee, and Hill 1960) was recently observed at 408 Mc/s and 1410 Mc/s by Mathewson and Rome (1963) with the 210-foot reflector in Australia. Flux densities of 6.8×10^{-26} MKS and 17.0×10^{-26} MKS are reported corresponding to a spectral index $\alpha = -0.7$. The radio source at 1410 Mc/s coincides within 0.1 m, and 0'.0 with the optical position of the nucleus revised by R. Shobbrook at Mount Stromlo. An unexpected result is that the angular diameter of the source could not be detected with the 14' beam at the higher frequency; hence it is presumed to be under 5' at half-intensity (the same conclusion was reached for NGC 253 and 5236). This is much less than the optical

TABLE 3

PHOTOMETRIC PARAMETERS OF NGC 1313

Apparent distance modulus (pg)	$m - M = 29.0$
Corrected distance modulus	$m_0 - M = 27.9$
Geometric distance (Mpc)	$\Delta = 3.8$
Integrated luminosity*	$L_T = 16.45$
Adopted sky unit†	$\mu_s = 12.89$
Total apparent magnitude (pg)	$m_T = 9.85$
Absolute magnitude	$M_T = -19.15$
Absolute luminosity ($\odot = 1$)	$\log \mathfrak{L} = 9.86$
Position angle (1875), major axis	$\theta = 42° \pm 1°$
Mean axis ratio b/a ($3'5 < a < 11'5$)	$q = 0.193$
Inclination ($q_0 \simeq 0.135$)	$i = 82° \pm 1°$
Threshold surface brightness‡	$\mu_m = 27.3 = 0.95\odot/\mathrm{pc}^2$
Major axis at threshold‡	$2a_m = 24' \pm 2' = 26.5$ kpc
Minor axis at threshold‡	$2b_m = 6' \pm 1' = 6.6$ kpc
Major axis at $\mu = 25.0$ mag sec^{-2}	$2a(25) = 19'.2 = 21.1$ kpc
Luminosity within $\mu = 25.0$ mag sec^{-2}	$k(25) = 0.925$
Gradient of exponential component	$G(a) = -0.13$ min^{-1} $= -0.12$ kpc^{-1}
Equivalent gradient of exp. comp.	$G(r^*) = -0.405$ min^{-1} $= -0.37$ kpc^{-1}
Peak brightness of exp. comp.	$\mu(0) = 21.5: = 200\odot/\mathrm{pc}^2$
Observed peak brightness‡	$\mu_0 = 21.75 = 1570\odot/\mathrm{pc}^2$
Parameters at $k = \frac{1}{4}$	
Semimajor axis	$a_1 = 2'.72 = 2.99$ kpc
Axis ratio	$q_1 = 0.20$
Equivalent radius	$r_1^* = 1'.13 = 1.46$ kpc
Surface brightness‡	$\mu_1 = 22.33 = 90\odot/\mathrm{pc}^2$
Parameters at $k = \frac{1}{2}$ (effective)	
Semimajor axis	$a_e = 4'.51 = 4.96$ kpc
Axis ratio	$q_e = 0.18$
Equivalent radius	$r_e^* = 2'.13 = 2.34$ kpc
Surface brightness‡	$\mu_e = 22.80 = 58\odot/\mathrm{pc}^2$
Mean surface brightness†	$\mu_e' = 13.49 = 73\odot/\mathrm{pc}^2$
Parameters at $k = \frac{3}{4}$	
Semimajor axis	$a_3 = 6'.34 = 6.96$ kpc
Axis	$q_3 = 0.20$
Equivalent radius	$r_3^* = 3'.08 = 3.39$ kpc
Surface brightness‡	$\mu_3 = 23\ 68 = 26.6\odot/\mathrm{pc}^2$
Concentration indices	$C_{21} = r_e^*/r_1^* = 1.60$; $C_{32} = r_3^*/r_e^* = 1.45$

* Sky units per square minute † Mag (pg) per square minute ‡ Mag (pg) per square second.

diameter $D_m \times d_m = 24' \times 6'$ (Sec. VI). Mathewson and Rome conclude that late-type galaxies do not have radio coronae of the type observed in M31. It should be noted, nevertheless, that the equivalent effective diameter of NGC 4945 is only $2r_e^* = 4'.26$ ($2a_e \times 2b_e = 9'.0 \times 1'.6$) and that a radio source having a surface intensity distributed as the optical emission might not be easily resolved with a 14′ beam (at half-power). In a previous comparison between the optical (red light) and radio emission (85 Mc/s) of the Large Magellanic Cloud (de Vaucouleurs 1957, 1960) the two distributions were shown to have precisely the same equivalent effective diameters $2r_e^* = 6°.0$. The ratio of the optical diameters LMC/N4945 is about 85; it is doubtful whether the continuum

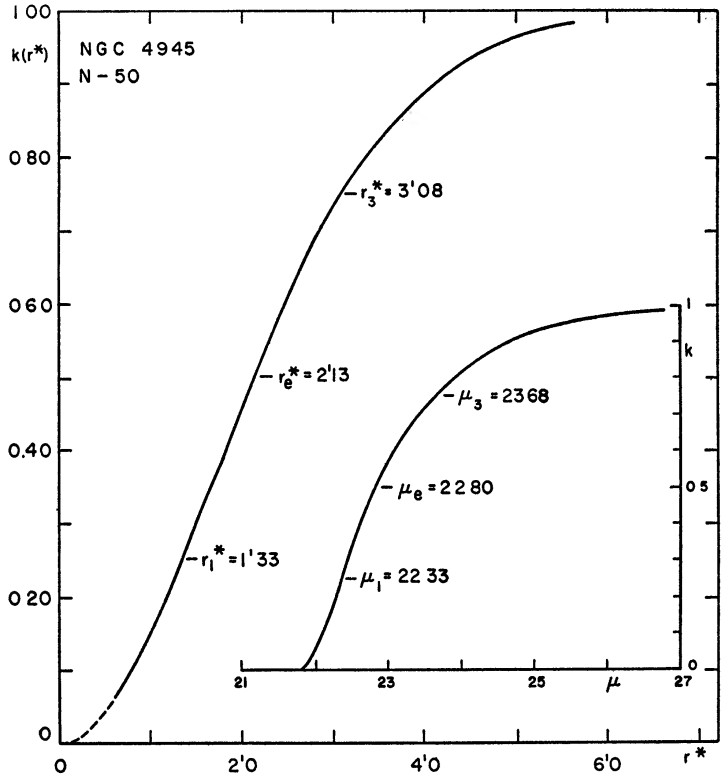

FIG. 9.—Relative integrated luminosity curve, $k(r^*) = L(r^*)/L_T$. *Inset:* k as a function of surface brightness μ. Half total luminosity is within equivalent effective radius $r_e^* = 2'13''$, where $\mu_e = 22.80$ mag sec^{-2}.

source in the Large Cloud would be resolved with a radio telescope having a $14' \times 85 \simeq 20°$ beam width at half-power. This discussion is not presented as an objection to the main conclusion of Mathewson and Rome, namely, that an extensive radio corona of the M31 type is not present in late-type galaxies, but merely to show that existing observations do not *require* that the continuum source be restricted to a small region or perhaps a point source near the center of the galaxy. An extended continuum source coextensive with the stellar system and moderately concentrated, such as is actually observed in the Large Cloud, is not excluded by the new Australian observations. The comparison of NGC 4945 with the Large Cloud is relevant since the morphological types are quite close, respectively SB(s)d and SB(s)m.

From the observed flux densities at 408 and 85 Mc/s an approximate value of $S = (13 \pm 4:) \times 10^{-26}$ MKS obtains at 159 Mc/s and the radio magnitude on the Jodrell Bank scale (Hanbury Brown 1962) is $m_r = -53.45 - 2.5 \log S = +8.75 \pm 0.3:$. By

comparison with the integrated photographic magnitude (Sec. VII) corrected for galactic absorption only $m_p - A = 9.85 - 1.1 = 8.75 \pm 0.3$:, the *apparent* radio index is $m_r - m_p = 0.0 \pm 0.45$:. Correction for internal absorption is uncertain; for type Sd and axis ratio $q = 0.2$, statistical data on colors (Holmberg 1958; de Vaucouleurs 1962) suggest a differential absorption (from the pole-on view) $\Delta A_i = 1.0$ mag. and total absorption $A_i = 1.2$ mag. The revised radio index corrected for both galactic and internal absorption then is $m_r - m_p = +1.3 \pm 0.5$: mag., which is about average for Sc–Sd galaxies (Hanbury Brown 1962).

It is a pleasure to acknowledge the help of Miss J. Page, who measured the plate and drew the complicated isophote chart at Harvard Observatory; and of Mrs. V. Rubin who provided valuable computer programming as part of the initial stages of her own galaxy photometry project, at Georgetown University Observatory. This continuing program is supported by the National Science Foundation.

REFERENCES

Elvey, T. C., and Roach, F. E. 1937, *Ap. J.*, **85**, 213.
Hanbury Brown, R. 1962, *Problems of Extragalactic Research*, I.A.U. Symposium No. 15 (New York: Macmillan), 79.
Holmberg, E. 1958, *Medd. Lund*, II, Nr. 136, 50.
Mathewson, D. S., and Rome, J. M. 1963, *Observatory*, **83**, 20.
Mills, B. Y. 1955, *Australian J. Phys.*, **8**, 368.
Mills, B. Y., Slee, O. B., and Hill, E. R. 1960, *ibid.*, **13**, 694.
Vaucouleurs, G. de. 1956*a*, *Occ. Notes R.A.S.*, No. 18.
———. 1956*b*, *Mem. Commonwealth Obs.*, Vol. **3**, No. 13.
———. 1957, *Radio Astronomy*, I.A.U. Symp. No. 4 (Cambridge: Cambridge University Press), p. 244.
———. 1960, *Ap. J.*, **131**, 584.
———. 1961, *ibid.*, **133**, 405. (Paper I.)
———. 1962, *Problems of Extragalactic Research*, I.A.U. Symposium No. 15 (New York: Macmillan Co), p. 3.
———. 1963*a*, *Ap. J.*, **137**, 720. (Paper III.)
———. 1963*b*, *ibid.*, **138**, 934. (Paper IV.)
Vaucouleurs, G. and A. de. 1961, *Mem. R.A.S.*, **68**, Part 3, 69.
———. 1963*a*, *Ap. J.*, **137**, 363.
———. 1963*b*, *A.J.*, **68**, 278.
Vaucouleurs, G. de, and Page, J. 1962, *Ap. J.*, **136**, 107. (Paper II.)